PAPER

Enhancing detection of steady-state visual evoked potentials using channel ensemble method

Journal of Neural Engineering

PAPER

Enhancing detection of steady-state visual evoked potentials using channel ensemble method

Wenqiang Yan[1,2,*], Chenghang Du[1], Dan Luo[1], YongCheng Wu[1], Nan Duan[1], Xiaowei Zheng[1] and Guanghua Xu[1,2,*]

[1] School of Mechanical Engineering, Xi'an Jiaotong University, Xi'an, People's Republic of China
[2] State Key Laboratory for Manufacturing Systems Engineering, Xi'an Jiaotong University, Xi'an, People's Republic of China
[*] Authors to whom any correspondence should be addressed.

E-mail: yanwenq@xjtu.edu.cn **and** ghxu@xjtu.edu.cn

RECEIVED
25 September 2020

REVISED
9 February 2021

ACCEPTED FOR PUBLICATION
18 February 2021

PUBLISHED
19 March 2021

Keywords: brain–computer interface, steady-state visual evoked potential, motion stimulus, training-free algorithm, channel ensemble

Abstract

Objective. This study proposed and evaluated a channel ensemble approach to enhance detection of steady-state visual evoked potentials (SSVEPs). *Approach.* Collected multi-channel electroencephalogram signals were classified into multiple groups of new analysis signals based on correlation analysis, and each group of analysis signals contained signals from a different number of electrode channels. These groups of analysis signals were used as the input of a training-free feature extraction model, and the obtained feature coefficients were converted into feature probability values using the *softmax* function. The ensemble value of multiple sets of feature probability values was determined and used as the final discrimination coefficient. *Main results.* Compared with canonical correlation analysis, likelihood ratio test, and multivariate synchronization index analysis methods using a standard approach, the recognition accuracies of the methods using a channel ensemble approach were improved by 5.05%, 3.87%, and 3.42%, and the information transfer rates (ITRs) were improved by 6.00%, 4.61%, and 3.71%, respectively. The channel ensemble method also obtained better recognition results than the standard algorithm on the public dataset. This study validated the efficiency of the proposed method to enhance the detection of SSVEPs, demonstrating its potential use in practical brain–computer interface (BCI) systems. *Significance.* A SSVEP-based BCI system using a channel ensemble method could achieve high ITR, indicating great potential of this design for various applications with improved control and interaction.

1. Introduction

Brain–computer interface (BCI) technology is an exciting focus of human–computer interaction and neural regulation work [1–3]. BCI has shown bright application prospects to improve the life quality of patients with amyotrophic lateral sclerosis, brain injury, and other neurological diseases. Among BCI methods [4–6], steady-state visual evoked potential (SSVEP) is one of the most promising technologies in the field because of its requirement of fewer recording electrodes, strong anti-interference ability, and high information transfer rate (ITR). The SSVEP-based BCI system uses a series of light-flashing or motion patterns with different frequencies as visual stimuli, where each stimulus pattern corresponds to an operation command [7–10]. Cerebral cortex activity is modulated when the user focuses on a certain stimulus pattern, and the occipital lobe of brain adopts the same periodic rhythm as the stimulus frequency. By detecting the main frequency components of the resulting electroencephalogram (EEG) induced by the stimulus pattern, the user's focused target can be identified so that the user's potential operation intention can be deduced.

The ITR is a generally accepted standard to evaluate the performance of BCI systems. Factors affecting the ITR include the number of stimulus targets, the recognition accuracy, and the time required for recognition. The number of stimulus targets is limited by the available frequencies of SSVEP and the monitor refresh rate [11, 12]. Therefore, researchers have

focused on the development efficient feature recognition algorithms to accurately identify focused targets in a short time and improve the ITR of SSVEP-BCI systems. The algorithms developed for SSVEP frequency feature detection can be divided into two categories: training-free recognition algorithms and subject-specific training recognition algorithms. The training-free method does not require multiple rounds of experiments to collect the training data of users. Representative training-free methods include power spectral density analysis (PSDA) [13], canonical correlation analysis (CCA) [14], likelihood ratio test (LRT) [15], multivariate synchronization index (MSI) [16], and filter bank CCA (FBCCA) [17]. PSDA is a single channel analysis method, which uses methods such as fast Fourier transform [18] and wavelet transform [19] to estimate the power values at the frequencies of interest for SSVEP detection. The CCA, LRT, MSI, and FBCCA methods are all multi-channel spatial filtering methods, and they can obtain better feature recognition effects than the PSDA method due to the full utilization of multi-channel EEG information. The brain electrical activity of a user can change greatly due to the complexity of brain nerve activity, visual fatigue, changes in the surrounding environment, and movement of electrodes, complicating interpretation of activity patterns. Additionally, EEG signals are highly subject-specific. Studies have shown that incorporating a users training data can reduce the interference of spontaneous background EEG activities on the SSVEP response [20]. Thus, researchers have proposed many subject-specific training methods to improve the accuracy of SSVEP detection. These training methods require multiple rounds of experiments to collect user training data, and the representative algorithms include combined-CCA [21], multi-way CCA [22], multi-set CCA [23], multilayer correlation maximization [24], common feature analysis [25], multivariate linear regression [26], and task-related component analysis [7]. Compared with training-free methods, the training methods can obtain higher recognition accuracy. However, these training methods may result in long and tiring training sessions, reducing the practicality of BCIs, particularly for long-term users. Therefore, it is important to explore high-performance training-free feature recognition algorithms for improved function of SSVEP.

By combining data information from multiple learners, ensemble learning [27] can provide significantly superior generalization performance than using data information from a single learner. This study builds on the benefit of ensemble learning to propose a channel ensemble method to improve the performance of a training-free method for SSVEP-based BCI. The channel Oz was used as the reference signal, and the collected multi-channel EEG data were classified into multiple groups of new analysis signal by calculating the correlation coefficients between the remaining channels and channel Oz. Next, offline performance was evaluated using a 35-target SSVEP dataset recorded from 15 subjects. For this offline performance evaluation, the channel ensemble method was applied to CCA, LRT, and MSI methods, and the resulting performances of the standard algorithms with and without channel ensemble method were compared. After determining the optimal stimulus duration, an online experiment was conducted using the proposed method. Besides, the performance of the channel ensemble method was also evaluated on a public dataset. The goal of this study was to demonstrate the efficacy of the channel ensemble based method for enhanced detection of SSVEPs.

2. Methods

2.1. Subjects

The offline experiment and online experiment were carried out separately. Fifteen subjects (ten females, mean age 23 years) participated in the offline experiment and 20 subjects (14 females, mean age 24 years) participated in the online experiment. There was no overlap between the participants in the two experiments and all the participants have normal color and visual perception.

All 35 subjects mentioned above had participated in a previous SSVEP test experiment conducted by our research group. In that experiment, we recruited 120 subjects. The responses to the SSVEP of all subjects were ranked according to the accuracy index. According to the ranking, 15 out of 120 subjects were selected at equal intervals to participate in the offline experiment of this study, and then 20 out of 105 subjects were selected at equal intervals to participate in the online experiment of this study. Since the selected participants included people with both good responses to the SSVEP (accuracy > 90%) and poor responses to the SSVEP (accuracy < 30%), the effectiveness of the feature recognition algorithm proposed in this study was able to fully verified. The experimental protocol was established according to the ethical guidelines of the Helsinki Declaration and was approved by the Human Ethics Committee of Xi'an Jiaotong University.

2.2. Stimulus design

A checkerboard of radial contraction–expansion motion was used as stimulus paradigm, as described previously [9]. The stimulus program was developed under MATLAB using the Psychphysics Toolbox. The stimulus paradigms were presented by a 24.5-inch liquid-crystal display monitor. The resolution and refresh rate of the monitor are 1920 × 1080 pixels and 144 Hz, respectively. As shown in figure 1, the stimuli were arranged in a 5 × 7 matrix, and the horizontal and vertical intervals between two neighboring stimuli were 100 pixels and 50 pixels, respectively. The stimulus pattern was a circle with a diameter of

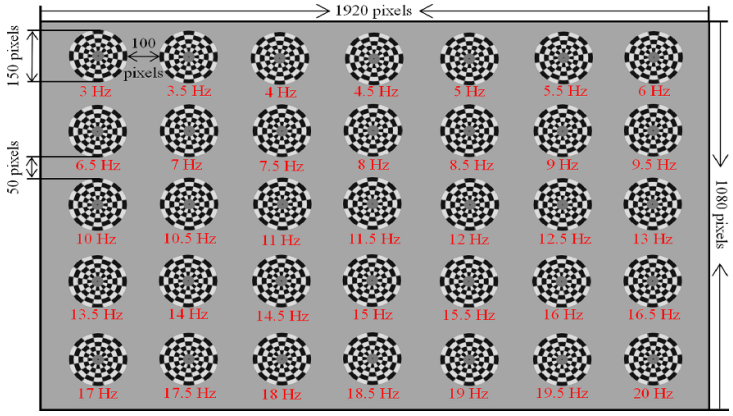

Figure 1. The frequencies of the 35 focused targets and their placements on the screen.

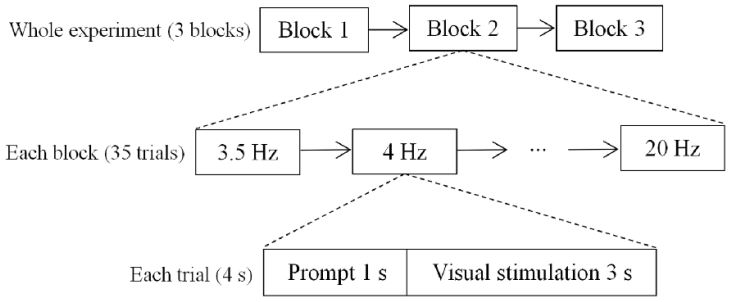

Figure 2. The flow chart of offline experiment.

150 pixels. The frequency range of 35 stimulus targets was 3–20 Hz with a frequency interval of 0.5 Hz. Since the single frequency component of the EEG is induced by motion stimulus [10], there can be multiple relationships between different target frequencies.

2.3. Data acquisition

A Neuracle system (NeuSenW) was used to collect the EEG. The sampling frequency of the equipment is 1000 Hz. An EEG amplifier and Triggerbox were combined to form the experimental platform. Event triggers generated by the Triggerbox were recorded on an event channel of the amplifier synchronized to the EEG data. The reference electrode was placed at the vertex (Cz), and the ground electrode was placed at the forehead (AFz). The EEGs were collected from the following eight channels: PO_5, PO_3, POz, PO_4, PO_6, O_1, Oz, and O_2.

2.4. Offline experiment

As shown in figure 2, the offline experiment consisted of three blocks. Each block contained 35 trials, and each trial lasted 3 s, separated by an interval of 1 s. Thirty-five targets were simultaneously presented on the monitor, and numbered 1–35. Before the stimulus begins, one of 35 serial numbers appeared below corresponding target indicating the focus target. Each subject was asked to shift their gaze to the focus target as soon as possible within 1 s. Between the two blocks, the subjects can rest properly. The subjects were 60–80 cm away from the monitor.

The corresponding EEG data segments were extracted in accordance with the event triggers. The MATLAB library function *detrend* was used to remove the linear trends for each channel. Considering a latency delay in the visual pathway, the first 130 sampling points of each channel were discarded when performing accuracy analysis on the extracted data.

2.5. Online experiment

The performance of the proposed method was verified on-line. As shown in figure 3, the online experiment included three blocks each containing 35 trials. Each trial lasted 2.6 s, including 1.6 s for visual stimulus and 1 s for gaze shifting. Each trial started with a visual cue (a red number) appeared below corresponding target indicating the focus target. Each time the serial number of the focused target identified by the proposed method was provided to the subject through the monitor. The other components of the design of the online experiment were the same as those of the offline experiment.

2.6. SSVEP detection algorithms

For the test signal $\boldsymbol{Y}\in R^{Nc\times Ns}$, N_c represents the number of channels and N_s represents the number

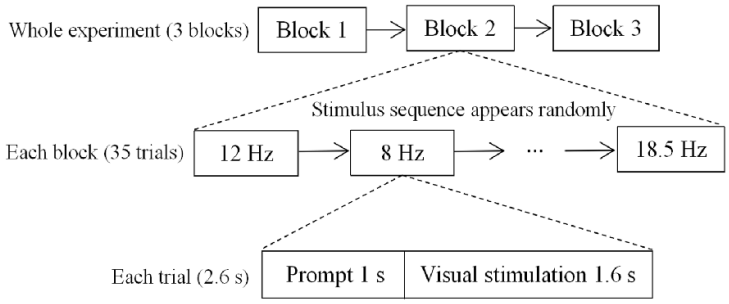

Figure 3. The flow chart of online experiment.

of sampling points. The SSVEP feature recognition algorithm aims to accurately detect the main frequency components $f \in \{f_1, f_2, \ldots, f_N\}$ in the test signal $\boldsymbol{Y}$, where f_i represents the stimulus frequency and N represents the number of stimulus targets. The SSVEP training-free feature recognition algorithm constructs reference signals ($\boldsymbol{X}_1$, …, $\boldsymbol{X}_f$, …, $\boldsymbol{X}_N$) at different stimulus frequencies, and then calculates the characteristic coefficient between the test signal $\boldsymbol{Y}$ and the reference signal $\boldsymbol{X}_f$ using the feature extraction model $\psi(\cdot)$. The frequency that corresponds to the largest characteristic coefficient is identified as the focused target frequency:

$$f^* = \arg\max_{f \in \{f_1, f_2, \ldots, f_N\}} \psi(\boldsymbol{Y}, \boldsymbol{X}_f). \tag{1}$$

2.7. Canonical correlation analysis

For two sets of multidimensional variable signals $\boldsymbol{X}$ and $\boldsymbol{Y}$, the goal of the CCA is to find two sets of linear projection vectors $\boldsymbol{w_X}$ and $\boldsymbol{w_Y}$, so that the correlation coefficient of the linear combinations $\boldsymbol{w_X}^{\mathrm{T}}\boldsymbol{X}$ and $\boldsymbol{w_Y}^{\mathrm{T}}\boldsymbol{Y}$ has the maximum value. The maximum canonical correlation coefficient of $\boldsymbol{X}$ and $\boldsymbol{Y}$ can be obtained by maximizing the following:

$$\max_{\boldsymbol{w_Y}, \boldsymbol{w_X}} \rho(\boldsymbol{Y}, \boldsymbol{X}) = \frac{E\left(\boldsymbol{w}_Y^T \boldsymbol{Y}\boldsymbol{X}^T \boldsymbol{w}_X\right)}{\sqrt{E\left(\boldsymbol{w}_Y^T \boldsymbol{Y}\boldsymbol{Y}^T \boldsymbol{w}_Y\right) E\left(\boldsymbol{w}_X^T \boldsymbol{X}\boldsymbol{X}^T \boldsymbol{w}_X\right)}}. \tag{2}$$

The multi-channel EEG data are denoted as $\boldsymbol{Y} = [\boldsymbol{Y}_1\ \boldsymbol{Y}_2\ \boldsymbol{Y}_3\ \ldots\ \boldsymbol{Y}_{NC}]^{\mathrm{T}}$, where N_C represents the channel number. The reference signal at the stimulus frequency f can be defined as:

$$\boldsymbol{X}_f = \begin{bmatrix} \cos 2\pi f t \\ \sin 2\pi f t \\ \cdots \\ \cos 2k\pi f t \\ \sin 2k\pi f t \end{bmatrix}, \quad t = 1/f_s, \ldots, N_s/f_s \tag{3}$$

where k represents the number of EEG harmonics, f_s is the sampling rate and N_s represents the number of sample points. By calculating the canonical correlation coefficients (ρ_1, ρ_2, …, ρ_N) between multichannel EEG data $\boldsymbol{Y}$ and the reference signals at all stimulus frequencies, and the maximum correlation coefficient is obtained and used as an SSVEP feature, represented by $\psi(\cdot)$ in equation (1).

2.8. Likelihood ratio test

For a p-dimensional normal distribution vector $\boldsymbol{Z} = [\boldsymbol{Z}_1; \boldsymbol{Z}_2]$, the dimensions of $\boldsymbol{Z}_1$ and $\boldsymbol{Z}_2$ are p_1 and p_2, respectively, and $p = p_1 + p_2$. Where $\boldsymbol{Z}_1 = \boldsymbol{Y}$, the multi-channel EEG data, and $\boldsymbol{Z}_2 = \boldsymbol{X}_f$, the reference signal at the stimulus frequency f. The mean matrix $\boldsymbol{\mu}$ and the covariance matrix $\boldsymbol{D}$ of $\boldsymbol{Z}$ can be expressed as:

$$\boldsymbol{\mu} = \begin{bmatrix} \boldsymbol{\mu}_1 \\ \boldsymbol{\mu}_2 \end{bmatrix}, \ \boldsymbol{D} = \begin{bmatrix} \boldsymbol{D}_{11} & \boldsymbol{D}_{12} \\ \boldsymbol{D}_{21} & \boldsymbol{D}_{22} \end{bmatrix}. \tag{4}$$

The null hypothesis of the two independent variables $\boldsymbol{Z}_1$ and $\boldsymbol{Z}_2$ can be written as follows:

$$H_0 : \boldsymbol{D}_{12} = 0, \ H_1 : \boldsymbol{D}_{12} \neq 0. \tag{5}$$

According to the LRT, the likelihood ratio statistic for equation (5) is as follows:

$$\lambda = \frac{\max_{H_0} L(\boldsymbol{\mu}, \boldsymbol{D})}{\max_{H_0 \cup H_1} L(\boldsymbol{\mu}, \boldsymbol{D})} = \frac{|\boldsymbol{D}|^{N_s/2}}{|\boldsymbol{D}_{11}|^{N_s/2} \cdot |\boldsymbol{D}_{22}|^{N_s/2}}. \tag{6}$$

The statistical measurement λ in equation (6) is represented as $\lambda = V^{Ns/2}$, where

$$V = \frac{|\boldsymbol{D}|}{|\boldsymbol{D}_{11}| \cdot |\boldsymbol{D}_{22}|} = \frac{\left|\boldsymbol{D}_{11} - \boldsymbol{D}_{12} \cdot \boldsymbol{D}_{22}{}^{-1} \cdot \boldsymbol{D}_{21}\right|}{|\boldsymbol{D}_{11}|} \tag{7}$$

V is a parameter to measure the distance between $\boldsymbol{Z}_1$ and $\boldsymbol{Z}_2$, where the correlation between the two is 1 V. Thus, the correlation between $\boldsymbol{Z}_1$ and $\boldsymbol{Z}_2$ can be expressed as:

$$C = 1 - \left(\frac{|\boldsymbol{D}|}{|\boldsymbol{D}_{11}| \cdot |\boldsymbol{D}_{22}|}\right)^{1/p_2}. \tag{8}$$

The range of C is (0, 1), meaning that $\boldsymbol{Z}_1$ and $\boldsymbol{Z}_2$ are independent when $C = 0$ and $\boldsymbol{Z}_1$ and $\boldsymbol{Z}_2$ are linearly related when $C = 1$. The correlation coefficients (C_1, C_2, …, C_N) between the multichannel EEG data $\boldsymbol{Y}$ and the reference signals for all stimulus frequencies can be estimated and used to compute the SSVEP features $\psi(\cdot)$ in equation (1).

2.9. Multivariate synchronization index

The MSI is used for feature extraction by estimating the synchronization index between the multi-channel EEG data $\boldsymbol{Y}$ and the reference signal $\boldsymbol{X}_f$. The correlation matrix $\boldsymbol{R}$ between $\boldsymbol{Y}$ and $\boldsymbol{X}_f$ is:

$$\boldsymbol{R} = \begin{bmatrix} \boldsymbol{R}_{11} & \boldsymbol{R}_{12} \\ \boldsymbol{R}_{21} & R_{22} \end{bmatrix} \tag{9}$$

where:

$$\boldsymbol{R}_{11} = \frac{1}{N_s}\boldsymbol{Y}\boldsymbol{Y}^T,\ \boldsymbol{R}_{22} = \frac{1}{N_s}\boldsymbol{X}_f\boldsymbol{X}_f^T,\ \boldsymbol{R}_{12} = \frac{1}{N_s}\boldsymbol{Y}\boldsymbol{X}_f^T,$$
$$\boldsymbol{R}_{21} = \frac{1}{N_s}\boldsymbol{X}_f\boldsymbol{Y}^T. \tag{10}$$

To reduce a potential influence of autocorrelation between $\boldsymbol{Y}$ and $\boldsymbol{X}_f$, the autocorrelation matrix in $\boldsymbol{R}$ is removed:

$$\boldsymbol{U} = \begin{bmatrix} \boldsymbol{R}_{11}{}^{-\frac{1}{2}} & 0 \\ 0 & \boldsymbol{R}_{22}{}^{-\frac{1}{2}} \end{bmatrix}. \tag{11}$$

The new correlation matrix $\boldsymbol{Q}$ after transformation is:

$$\boldsymbol{Q} = \boldsymbol{U}\boldsymbol{R}\boldsymbol{U}^T = \begin{bmatrix} \boldsymbol{I}_{N_C \times N_C} & \boldsymbol{R}_{11}{}^{-\frac{1}{2}}\boldsymbol{R}_{12}\boldsymbol{R}_{22}{}^{-\frac{1}{2}} \\ \boldsymbol{R}_{22}{}^{-\frac{1}{2}}\boldsymbol{R}_{21}\boldsymbol{R}_{11}{}^{-\frac{1}{2}} & \boldsymbol{I}_{2N_h \times 2N_h} \end{bmatrix} \tag{12}$$

where N_C represents the number of channels and N_h represents the number of harmonics of the reference signal. Let $\lambda_1, \lambda_2, \ldots, \lambda_m$ represent the eigenvalues of the matrix $\boldsymbol{Q}$, which are normalized as follows:

$$\lambda'_i = \frac{\lambda_i}{\sum_{i=1}^{m}\lambda_i} = \frac{\lambda_i}{\mathrm{tr}(\boldsymbol{Q})} \tag{13}$$

where $m = N_c + 2N_h$. The synchronization index S between $\boldsymbol{Y}$ and $\boldsymbol{X}_f$ can be expressed as:

$$S = 1 + \frac{\sum_{i=1}^{m}\lambda'_i \log(\lambda'_i)}{\log(m)}. \tag{14}$$

According to equation (14), when two sets of signals are completely uncorrelated, i.e. $\boldsymbol{R}_{12} = \boldsymbol{R}_{21} = 0$, then $\boldsymbol{Q}$ is a diagonal matrix, $\lambda_i' = 1/m$ and $S = 0$. When two sets of signals are completely correlated, then $\lambda_i' = 1$, and the other normalized eigenvalues are 0 and $S = 1$. The synchronization indexes $(S_1, S_2, \ldots, S_N)$ between the multichannel EEG data $\boldsymbol{Y}$ and the reference signals at all stimulus frequencies can be obtained and used as the SSVEP features $\psi(\cdot)$ in equation (1).

2.10. Channel ensemble based method

The EEG data channel has an important influence on SSVEP feature recognition. To fully utilize the effective information contained in different channel combinations, a channel ensemble method was developed. As shown in figure 4, this approach mainly includes the following steps:

2.10.1. Channel signals division

For SSVEP, the Oz channel usually has the strongest response [28]. Therefore, the Oz channel was selected as the reference channel here, and the correlation coefficients between the remaining channel signals and the Oz channel signal $\boldsymbol{Y}^{\mathrm{Oz}}$ were then calculated:

$$e_i = \frac{\sum_{j=1}^{N_s}(\boldsymbol{Y}_j^{Oz} - \overline{\boldsymbol{Y}^{Oz}})(\boldsymbol{Y}_j^i - \overline{\boldsymbol{Y}^i})}{\sqrt{\sum_{j=1}^{N_s}(\boldsymbol{Y}_j^{Oz} - \overline{\boldsymbol{Y}^{Oz}})^2}\sqrt{\sum_{j=1}^{N_s}(\boldsymbol{Y}_j^i - \overline{\boldsymbol{Y}^i})^2}} \tag{15}$$

where N_s represents the number of sampling points, and $i \in \{\mathrm{PO_5}, \mathrm{PO_3}, \mathrm{POz}, \mathrm{PO_4}, \mathrm{PO_6}, \mathrm{O_1}, \mathrm{O_2}\}$. According to the order of the calculated correlation coefficients $\{e_{\mathrm{PO5}}, e_{\mathrm{PO3}}, e_{\mathrm{POZ}}, e_{\mathrm{PO4}}, e_{\mathrm{PO6}}, e_{\mathrm{O1}}, e_{\mathrm{O2}}\}$ from largest to smallest, the corresponding channel signals $\{\boldsymbol{Y}^{\mathrm{PO5}}, \boldsymbol{Y}^{\mathrm{PO3}}, \boldsymbol{Y}^{\mathrm{POz}}, \boldsymbol{Y}^{\mathrm{PO4}}, \boldsymbol{Y}^{\mathrm{PO6}}, \boldsymbol{Y}^{\mathrm{O1}}, \boldsymbol{Y}^{\mathrm{O2}}\}$ were reordered as $\{\boldsymbol{L}_1, \boldsymbol{L}_2, \ldots, \boldsymbol{L}_7\}$. Among them, the correlation coefficient between $\boldsymbol{L}_1$ and $\boldsymbol{Y}^{\mathrm{Oz}}$ is the largest, and the correlation coefficient between $\boldsymbol{L}_7$ and $\boldsymbol{Y}^{\mathrm{Oz}}$ is the smallest. Then the multi-channel EEG signals were classified into seven groups of channel signals: $\{\boldsymbol{Y}^{\mathrm{Oz}}, \boldsymbol{L}_1\}$, $\{\boldsymbol{Y}^{\mathrm{Oz}}, \boldsymbol{L}_1, \boldsymbol{L}_2\}$, $\{\boldsymbol{Y}^{\mathrm{Oz}}, \boldsymbol{L}_1, \boldsymbol{L}_2, \boldsymbol{L}_3\}$, $\{\boldsymbol{Y}^{\mathrm{Oz}}, \boldsymbol{L}_1, \boldsymbol{L}_2, \boldsymbol{L}_3, \boldsymbol{L}_4\}$, $\{\boldsymbol{Y}^{\mathrm{Oz}}, \boldsymbol{L}_1, \boldsymbol{L}_2, \boldsymbol{L}_3, \boldsymbol{L}_4, \boldsymbol{L}_5\}$, $\{\boldsymbol{Y}^{\mathrm{Oz}}, \boldsymbol{L}_1, \boldsymbol{L}_2, \boldsymbol{L}_3, \boldsymbol{L}_4, \boldsymbol{L}_5, \boldsymbol{L}_6\}$, and $\{\boldsymbol{Y}^{\mathrm{Oz}}, \boldsymbol{L}_1, \boldsymbol{L}_2, \boldsymbol{L}_3, \boldsymbol{L}_4, \boldsymbol{L}_5, \boldsymbol{L}_6, \boldsymbol{L}_7\}$.

2.10.2. Feature extraction

For each group of channel signals, the feature extraction model $\psi(\cdot)$ introduced in the CCA, LRT, or MSI method was used to calculate the characteristic coefficients. Each group of channel signals can generate N characteristic coefficients $(\delta_1, \delta_2, \ldots, \delta_N)$, where N represents the number of stimulus frequencies. The *softmax* function can normalize the vector, highlight the largest value, and suppress other components far below the maximum value to enhance the needed information. Thus, the calculated N characteristic coefficients were transformed into characteristic probability values by *softmax* function:

$$\delta_i' = \frac{e^{\delta_i}}{\sum_{j=1}^{N} e^{\delta_j}}. \tag{16}$$

The characteristic probability values of the seven groups of channel signals obtained after the same operation were recorded as matrix $\boldsymbol{A}$, with dimensions of $N \times 7$, where each row corresponds to a stimulus frequency f and each column corresponds to a group of channel signals.

2.10.3. Channel signals features ensemble

For SSVEP, the use of multi-channel EEG information allows better recognition effect. Therefore, the proportion of the number of channels contained in each group of channel signals to the total number of

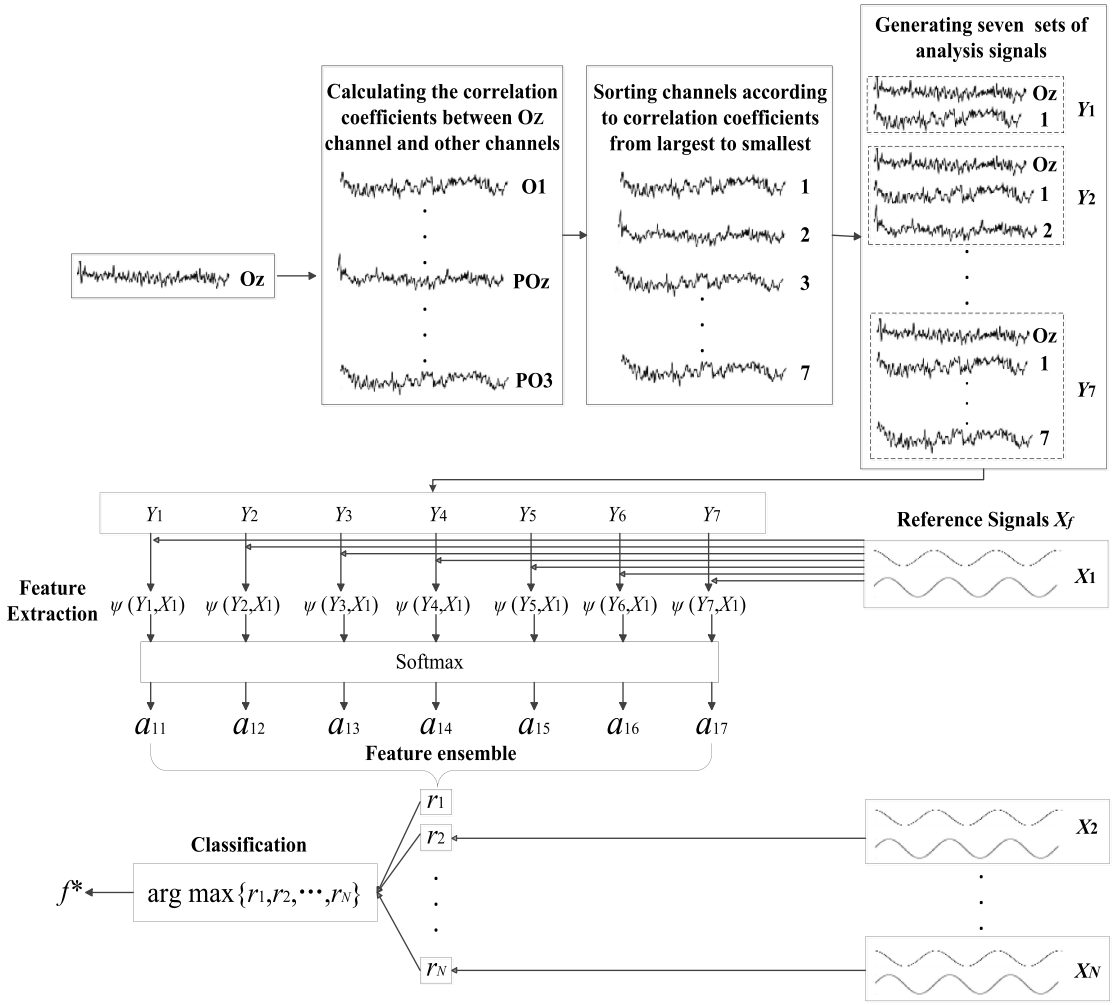

Figure 4. The algorithm flow of channel ensemble method.

channels (i.e. 8) was used as the weight of the channel signals features ensemble. The ensemble characteristic coefficients were obtained as follows:

$$r_i = \sum_{j=2}^{Nc} \frac{j}{N_c} \cdot a_{ij} \tag{17}$$

where N_c represents the number of channels, and a_{ij} represents the feature probability value in matrix $\boldsymbol{A}$.

2.10.4. Feature recognition

The frequency corresponding to the maximum value among the calculated N characteristic coefficients (r_1, r_2, …, r_N) was used as the focused target frequency:

$$f^* = \arg\max\{r_1, r_2, \ldots, r_N\}. \tag{18}$$

The procedure of calculating the ensemble coefficient of EEG signal $\boldsymbol{Y}$ at the stimulation frequency f by channel ensemble method is shown in figure 5. By calculating the ensemble coefficients of $\boldsymbol{Y}$ at all frequencies, the frequency corresponding to the maximum coefficient was defined as the target frequency.

3. Results

3.1. Analysis of the influence of channels on the accuracy of feature recognition

The accuracy analyses of multiple groups of channel signals described in section 2.10 were carried out. Since the FBCCA method is suitable for the analysis of multi-harmonic EEG signals [17], and there is no harmonic in EEG induced by motion stimulus paradigm [10]. Thus, the CCA, LRT and MSI methods other than the FBCCA method were used as standard algorithms in this study. Figures 6(a)–(c) show the recognition accuracy results for three subjects under different channel signals obtained separately using CCA, LRT and MSI methods, respectively, for analysis of 1.2 s of data length. The experimental results of the three methods showed that channels had an important influence on SSVEP feature recognition, with significant fluctuation in the recognition accuracy of the different channel signals. Therefore, it is obvious that a suitable channel ensemble method is required to improve the stability of the feature recognition algorithm.

Channel ensemble method: Channel_ensemble[Y, X_f, $\psi(\cdot)$]
Input: Y: EEG signal;
X_f: Reference signal at stimulus frequency f;
$\psi(\cdot)$: CCA/LRT/MSI feature recognition model.
Procedure:
1: **for** i=1, 2, ..., 7 do
2: Calculating the correlation coefficients e_i between $\{Y^{PO5}, Y^{PO3}, Y^{POz}, Y^{PO4}, Y^{PO6}, Y^{O1}, Y^{O2}\}$ and Y^{Oz} using Eq.(15);
3: **end for**
4: According to the order of the correlation coefficients $\{e_{PO5}, e_{PO3}, e_{POZ}, e_{PO4}, e_{PO6}, e_{O1}, e_{O2}\}$ from largest to smallest, the corresponding channel signals $\{Y^{PO5}, Y^{PO3}, ..., Y^{O1}, Y^{O2}\}$ were reordered as $\{L_1, L_2, ..., L_7\}$;
5: Channel signals re-division: M_1:$\{Y^{Oz}, L_1\}$, M_2:$\{Y^{Oz}, L_1, L_2\}$, M_3:$\{Y^{Oz}, L_1, L_2, L_3\}$, M_4:$\{Y^{Oz}, L_1, L_2, L_3, L_4\}$, M_5:$\{Y^{Oz}, L_1, L_2, L_3, L_4, L_5\}$, M_6:$\{Y^{Oz}, L_1, L_2, L_3, L_4, L_5, L_6\}$, M_7:$\{Y^{Oz}, L_1, L_2, L_3, L_4, L_5, L_6, L_7\}$;
6: **for** j=1, 2, ..., 7 do
7: $\delta_j \leftarrow \psi(M_j, X_f)$;
8: **end for**
9: Calculating characteristic probability δ_j' of δ_j using Eq. (16);
10: Calculating ensemble characteristic coefficient r_f using Eq.(17).
Output: The ensemble coefficient r_f of EEG signal Y at stimulus frequency f.

Figure 5. The pseudo-code of the channel ensemble method.

As shown in figure 6, the channel signal with the best recognition accuracy differed for different subjects. For example, in the first block of the offline experiment, subject 1 exhibited the best recognition effect under channel signal 1, subject 2 exhibited the best recognition effect under channel signal 5, and subject 3 exhibited the best recognition effect under channel signal 4. There was variability even for the same subject, the channel signal with the best recognition effect between different blocks was also different. For example, for subject 1, the recognition effect of channel signal 1 was the best in the first block, but the effect of channel signal 7 was the best in the second block, and that of channel signal 6 was the best in the third block. In addition, the experimental results of the three methods showed that the recognition effect was not strictly correlated to the number of channels (i.e. eight channels did not always give the best recognition effect, and two channels did not always give the worst recognition effect). This variability may reflect the movement of the subject's body during the experiment, which can cause movement of the electrode.

The results show that the channel signal that obtains the best recognition effect may be different for different trials. The channel ensemble method can simultaneously use multiple sets of channel signal information, which can be considered to improve the performance of SSVEP feature recognition.

3.2. Comparison of offline performance between channel ensemble method and standard method

To test the effectiveness of the proposed method, the channel ensemble method was applied to the CCA, LRT, and MSI methods (see section 2.10 for the algorithm flow). The off-line experimental data were used to calculate the average recognition accuracies and ITRs for 15 subjects under different stimulus duration. Figure 7 shows the analysis results of CCA, LRT, and MSI methods with the channel ensemble algorithm and the standard algorithm.

As shown in figure 7, the channel ensemble method resulted in better recognition effect than the standard algorithm for all three methods, verifying its effectiveness. The paired t test results showed that when the stimulus duration was short (<2 s), the proposed method significantly improved the performance of the standard algorithm ($p < 0.05$). With increased stimulus duration, the performance of the standard algorithm and the channel ensemble method gradually become more similar. Considering that the SSVEP-BCI system usually requires a feature recognition algorithm to accurately identify the focused target in a short time, the excellent performance of the channel ensemble method for stimuli of short duration should facilitate its application in an actual BCI system.

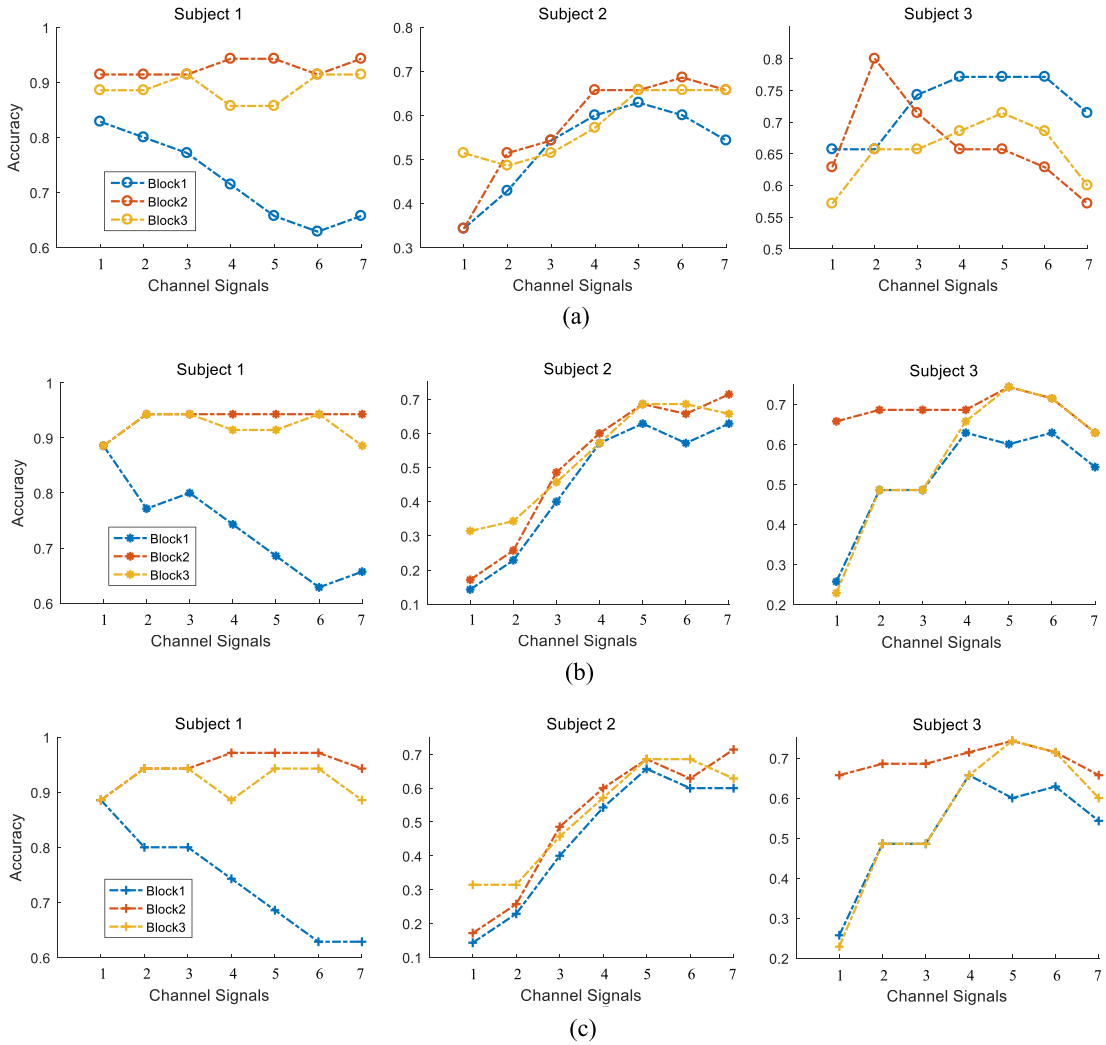

Figure 6. (a) Recognition accuracy for CCA under different channel signals. (b) Recognition accuracy for LRT under different channel signals. (c) Recognition accuracy for MSI under different channel signals.

The experimental results also showed increased recognition accuracy with the increase of stimulus duration. The ITR increased at first and then decreased with the increase of stimulus duration. With increased stimulus duration, the EEG gradually became steady and exhibited the same periodic rhythmic components as the stimulus frequency, for gradually increased recognition accuracy. The ITR is directly proportional to the accuracy, but inversely proportional to the stimulus duration. Therefore, in order to achieve the high ITR of an SSVEP-BCI system and avoid user visual fatigue caused by long-term use, the stimulus duration of SSVEP is usually limited to duration of less than 3 s. The experimental results in figure 7 showed that algorithms with either the channel ensemble or standard methods achieved the highest ITR for a stimulus duration of 1.6 s. Therefore, the stimulus duration of each trial was set to 1.6 s in the online experiment.

3.3. Online BCI performance

Figure 8 show the recognition accuracies and ITRs of 20 subjects under the channel ensemble and standard algorithms (CCA, LRT, and MSI). The 20 subjects participating in the online experiment included both participates who responded well to SSVEP and those who responded poorly to SSVEP (see section 2.1).

The experimental results presented in figure 8 show that the channel ensemble method proposed in this study resulted in a more obvious improvement effect for subjects with poor SSVEP response. As shown in figure 8, after applying the channel ensemble method to CCA, LRT, and MSI methods, almost all of the last 15 subjects obtained better recognition effect under the channel ensemble method. The recognition accuracies and the ITRs of the 20 subjects were superimposed and averaged, and the results are shown in figure 9. For the CCA method, the accuracy and ITR of the channel ensemble method were increased by 5.05%

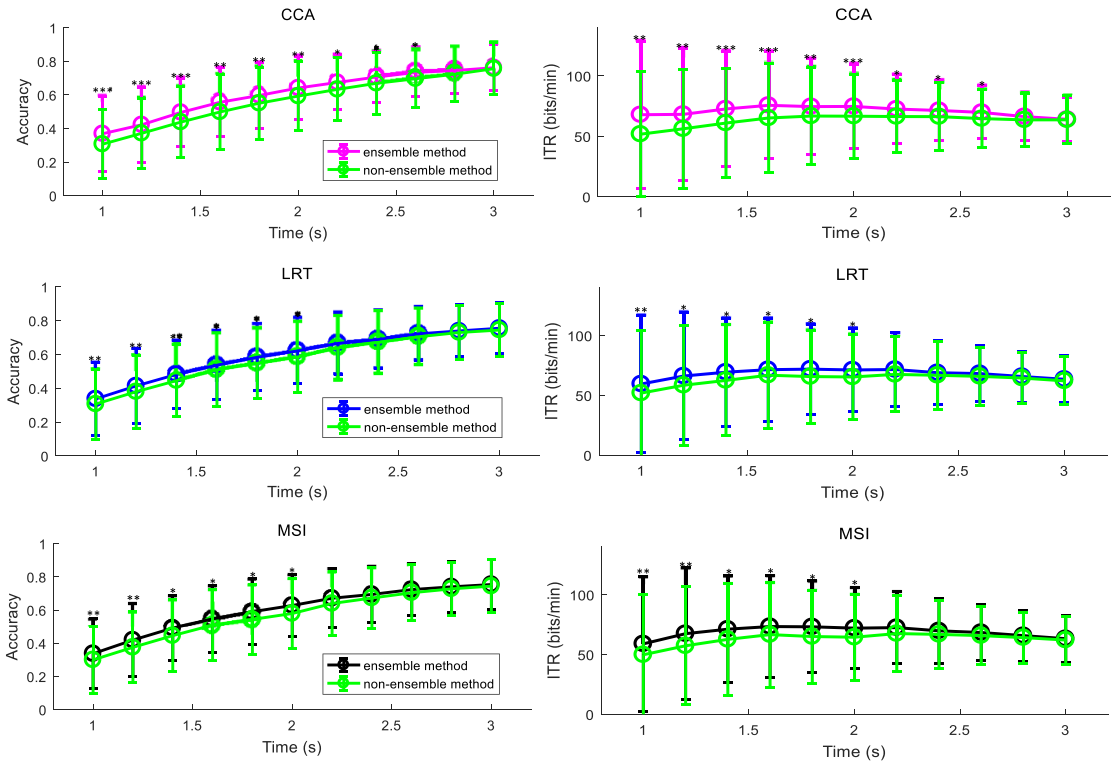

Figure 7. The average recognition accuracies and ITRs for CCA, LRT, and MSI methods with the channel ensemble algorithm and the standard algorithm. $^{***}p < 0.001$ between the two methods, $^{**}p < 0.01$ between the two methods, $^{*}p < 0.05$ between the two methods.

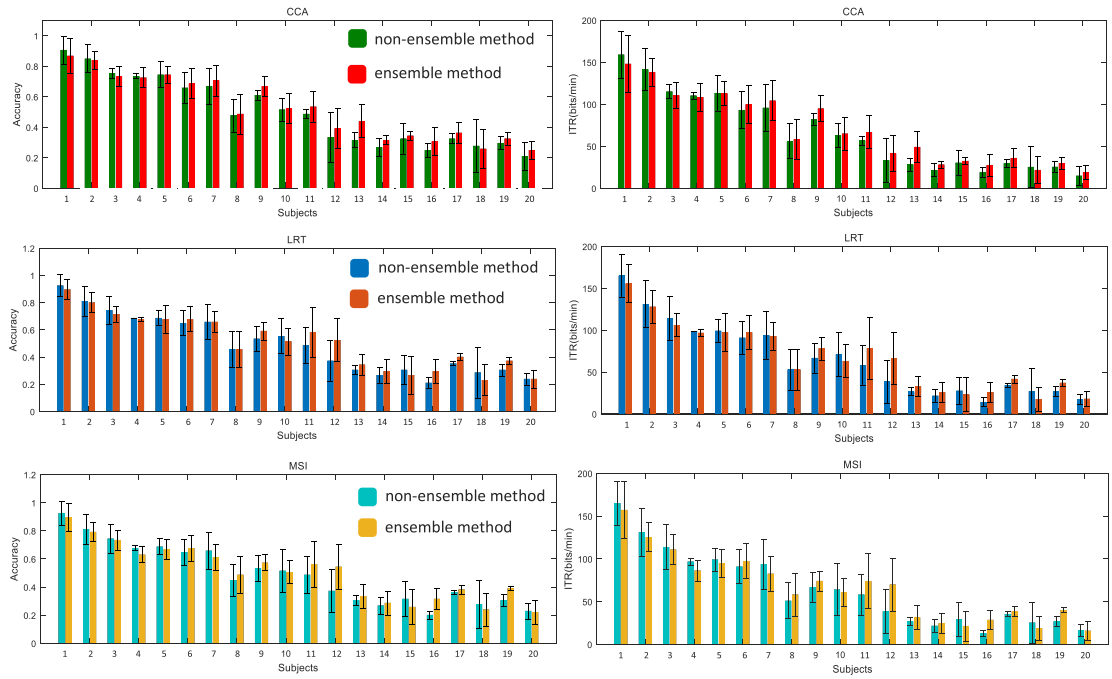

Figure 8. The recognition accuracies and ITRs of 20 subjects under the channel ensemble and standard algorithms.

and 6.00% respectively compared with the standard method, with a significant performance difference between the two. Similarly, for LRT method, the accuracy and ITR were increased by 3.87% and 4.61%, respectively, using the channel ensemble method compared with the standard method, and for MSI method, the accuracy and ITR of the channel ensemble method were increased by 3.42% and

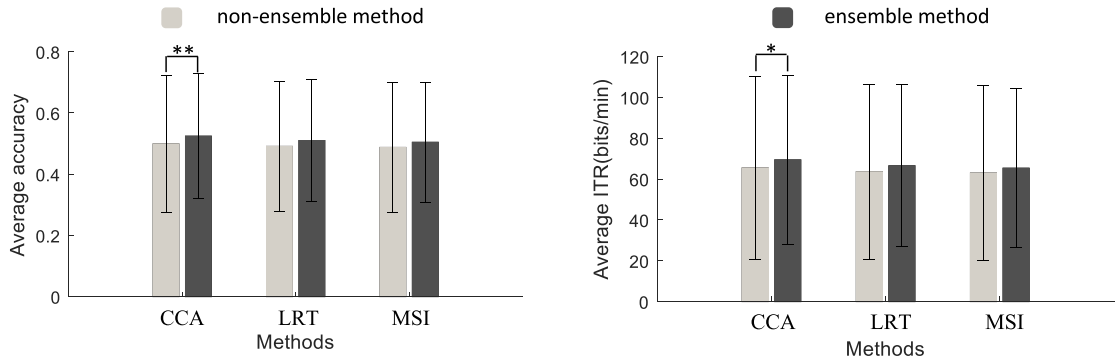

Figure 9. The average recognition accuracies and ITRs of 20 subjects under the channel ensemble and standard algorithms. $^{**}p < 0.01$ between the two methods, $^{*}p < 0.05$ between the two methods.

3.71%, respectively, compared with the standard method.

3.4. Analysis of validation results of channel ensemble method on public dataset

To further verify the effectiveness of the proposed method, the channel ensemble method was verified on a public dataset. The dataset is freely available on http://bci.med.tsinghua.edu.cn/download.html. This dataset gathered SSVEP-BCI recordings of 35 healthy subjects focusing on 40 characters flickering at different frequencies (8–15.8 Hz with an interval of 0.2 Hz). For each subject, the experiment consisted of six blocks. Each block contained 40 trials corresponding to all 40 characters indicated in a random order. SSVEP signals in the public dataset were induced by light-flashing paradigm and contained multiple harmonics. In this section, FBCCA, which is suitable for multi-harmonic SSVEP analysis, was used as the standard algorithm. The detailed information of the dataset can be found in Wang *et al* [29].

The accuracies of FBCCA and ensemble FBCCA (FBCCA combined with channel ensemble) were compared. For FBCCA method, the number of harmonics of the reference signals was set to 3, and the number of filter sub-bands was also set to 3 according to the filter setting method in Chen *et al* [17]. The analysis data length used in this study was 1.5 s and EEG data from eight channels (PO5, PO3, POz, PO4, PO6, O1, Oz, and O2) were analyzed.

Table 1 shows the average accuracies of 34 subjects (the data file of subject 5 in the public dataset was damaged and could not be downloaded) in six blocks using FBCCA and ensemble FBCCA methods, respectively. It can be seen from table 1 that 20 subjects obtained higher accuracy under the ensemble FBCCA method, and two subjects obtained the same accuracy under the two methods. The above results indicate that the ensemble FBCCA method is effective for most subjects in the public dataset. The experimental results also show that the ensemble FBCCA method did not significantly improve the accuracy of FBCCA method. All subjects in table 1 used the same reference channel (O1). The accuracies of 34 subjects at different reference channels were calculated, and the accuracy results of 34 subjects using their optimal reference channels instead of the fixed reference channel are shown in table 2. As can be seen from table 2, the average accuracy of the ensemble FBCCA method was 5.37% higher than that of the standard FBCCA method after optimizing the reference channel of the subjects, and there was a significant difference in the accuracy between the two methods ($p < 0.01$). Although the performance of the standard algorithm could still be improved when the fixed channel was used as reference channel for all subjects, the performance improvement is limited since different stimulus paradigm and EEG acquisition equipment were used between public dataset and this study. According to the accuracy results of subjects using fixed reference channel and their respective optimal reference channels in the public dataset, we recommend that researchers who use different EEG acquisition equipment from this study should conduct offline experiments first and choose appropriate reference channel for the subjects to obtain better recognition results.

4. Discussion

Compared with training-free feature recognition methods, the training methods require a lengthy and potentially tedious training process, which reduces the practicability of BCI systems, and may cause visual fatigue of users. Therefore, the goal of this study was to improve the performance of existing SSVEP training-free feature recognition algorithms. The experimental results showed that channel affected the feature recognition of SSVEP. Due to the movement of electrodes during the experiment, the recognition effect was not strictly correlated with the number of channels, so more channels are not always better. In addition, the channel signal for best recognition effect for a specific subject was not necessarily the same in each trial. The channel ensemble method proposed here utilized information from multiple groups of

Table 1. The average accuracies of 34 subjects in six blocks using FBCCA and ensemble FBCCA methods.

Subject	FBCCA	Ensemble FBCCA	Subject	FBCCA	Ensemble FBCCA	Subject	FBCCA	Ensemble FBCCA
S1	0.6417	0.6292	S14	0.7292	0.7250	S26	0.9083	0.9083
S2	0.7500	0.7708	S15	0.4208	0.4292	S27	0.8708	0.8708
S3	0.9500	0.9458	S16	0.4667	0.3875	S28	0.8333	0.8375
S4	0.8375	0.8625	S17	0.4667	0.5292	S29	0.3875	0.4250
S6	0.7583	0.8250	S18	0.6792	0.6542	S30	0.7042	0.7250
S7	0.7083	0.6833	S19	0.2292	0.2542	S31	0.7958	0.7458
S8	0.3250	0.3583	S20	0.7583	0.7667	S32	0.9333	0.9542
S9	0.6792	0.6083	S21	0.7792	0.8375	S33	0.4542	0.4792
S10	0.6083	0.6167	S22	0.9083	0.9125	S34	0.8083	0.8125
S11	0.1792	0.1500	S23	0.8208	0.8500	S35	0.6458	0.6417
S12	0.9292	0.9125	S24	0.7708	0.7917			
S13	0.6125	0.6792	S25	0.9375	0.9333			
Average			FBCCA: 0.6849		Ensemble FBCCA: 0.6915			

Table 2. The average accuracies of 34 subjects in six blocks using ensemble FBCCA method under their respective optimal reference channels.

Subject	Ensemble FBCCA	Reference channel	Subject	Ensemble FBCCA	Reference channel	Subject	Ensemble FBCCA	Reference channel
S1	0.6417	PO5	S14	0.7583	PO6	S26	0.9125	PO3
S2	0.7708	O1	S15	0.4583	O2	S27	0.8792	O2
S3	0.9542	PO6	S16	0.5083	PO6	S28	0.8625	Oz
S4	0.8625	O1	S17	0.5583	Oz	S29	0.4417	PO5
S6	0.8250	O1	S18	0.6917	PO4	S30	0.7583	O2
S7	0.6833	O1	S19	0.2750	Oz	S31	0.8333	O2
S8	0.4000	O2	S20	0.7833	PO5	S32	0.9500	PO5
S9	0.6500	PO4	S21	0.8375	PO3	S33	0.5042	PO3
S10	0.6292	Oz	S22	0.9125	O1	S34	0.8292	O2
S11	0.2083	PO6	S23	0.8500	PO5	S35	0.6500	PO6
S12	0.9292	POz	S24	0.8000	PO5			
S13	0.6833	PO5	S25	0.9417	PO5			
Average				Ensemble FBCCA: 0.7386				

channel signals and improved the stability of feature recognition algorithms. The channel ensemble method was applied to CCA, LRT, and MSI methods, and better recognition results were obtained for the proposed method compare to the standard algorithm for all three methods. An additional advantage is that the method proposed here can be used directly for any subject without the need for selection of parameters, as a completely training-free method.

Online experimental results revealed an obvious improvement effect for this method for subjects with poor SSVEP response and a general improvement effect for subjects with better SSVEP response. Subjects with better response tend to use all the electrode channels, while the subjects with poor response did not suitable to use all the electrode channels. This may be because the subjects with better responses activated more brain regions, making it more beneficial to fully utilize the multi-channel EEG information, while subjects with poor responses activated fewer brain regions, and the electrode channel for the best recognition effect needs to be optimized among multiple channels. The cause of the individual differences in SSVEP responses have not yet been determined, and this issue deserves further study. Subjects with poor SSVEP response exhibited greater improvement, which could make SSVEP-BCI applications more popular. The method proposed in this study effectively improved the recognition effect of poor response subjects, and showed a positive significance to promote the application of the SSVEP-BCI system.

Three standard feature recognition algorithms, CCA, LRT, and MSI, were tested in this study. Among them, CCA showed the best performance with both the standard and the ensemble methods, which is different from what was observed in previous studies [15, 16]. This may reflect differences due to the motion stimulus paradigm adopted in this study. Compared with light-flashing stimulus, EEG induced by motion stimulus contains fewer harmonic components, so there can be multiple relationships among the 35 stimulus frequencies set in this study. The use of a single harmonic can help increase the number of BCI coding targets, but does not promote feature recognition. Therefore, the accuracy calculated in this study was lower than the accuracy calculated in studies [7, 8] using light-flashing stimulus. Ensuring

the comfort of the paradigm required reducing the intensity of the paradigm stimulus, which reduces the signal-to-noise ratio of the induced EEG. Therefore, a more effective feature recognition algorithm is needed for motion stimulus. The method proposed and tested in this study showed excellent performance under motion stimulus and can be considered for use in actual BCI systems. The performance of the proposed method was also verified on the public dataset using light-flashing as stimulus paradigm. The results also show that the channel ensemble method is effective for improving SSVEP frequency detection performance.

Channel ensemble method used the fixed reference channel for all subjects, but the reference channel used may not necessarily be the best choice in each trial. In future research, we will investigate an adaptive reference channel selection method instead of using a fixed electrode as the reference channel to further improve the performance of the proposed method. Besides, we noticed that the EEG acquisition equipment has an impact on the channel ensemble method. We recommend that researchers who use different EEG acquisition equipment from this study should conduct offline experiments first to calculate the accuracy at different reference channels and choose appropriate reference channel for the subjects to obtain better recognition results. In addition, in the channel ensemble process, the ratio of the number of channels contained in the current channel signal to the total number of channels was used as the weighting factor, so a channel signal with more channels weighted more. An improved weighting strategy should be optimized in the next study. Overall, the performance of the algorithm proposed in this study can be further improved.

5. Conclusion

A novel SSVEP detection method using a channel ensemble approach was proposed and evaluated in this study. Compared with standard CCA, LRT, and MSI methods, the recognition accuracies of the channel ensemble method were increased by 5.05%, 3.87%, and 3.42%, and the ITRs were increased by 6.00%, 4.61%, and 3.71%, respectively. Especially for subjects with poor SSVEP response, the method proposed in this study effectively improved recognition performances. The effectiveness of the channel ensemble method was further verified on the public dataset. The performance of the proposed method was verified in a variety of methods and with multiple subjects, and could be applied for use in a practical BCI system.

Data availability statement

The data that support the findings of this study are available upon reasonable request from the authors.

Acknowledgments

This research was supported by China National Postdoctoral Program for Innovative Talents (No. BX20200273).

ORCID iDs

Wenqiang Yan https://orcid.org/0000-0002-2179-6023
Guanghua Xu https://orcid.org/0000-0002-1294-4741

References

[1] Anumanchipalli G K, Chartier J and Chang E F 2019 Speech synthesis from neural decoding of spoken sentences *Nature* **568** 493–8
[2] Heelan C *et al* 2019 Decoding speech from spike-based neural population recordings in secondary auditory cortex of non-human primates *Commun. Biol.* **2** 466
[3] Kubanek J, Brown J, Ye P, Pauly K B, Moore T and Newsome W 2020 Remote, brain region–specific control of choice behavior with ultrasonic waves *Sci. Adv.* **6** eaaz4193
[4] Edelman B J, Meng J, Suma D, Zurn C, Nagarajan E, Baxter B S, Cline C C and He B 2019 Noninvasive neuroimaging enhances continuous neural tracking for robotic device control *Sci. Rob.* **4** eaaw6844
[5] Li W, Li M, Zhou H, Chen G, Jin J and Duan F 2018 A dual stimuli approach combined with convolutional neural network to improve information transfer rate of event-related potential-based brain-computer interface *Int. J. Neural Syst.* **28** 185003
[6] Oikonomou V P, Nikolopoulos S and Kompatsiaris I 2019 A Bayesian multiple kernel learning algorithm for SSVEP BCI detection *IEEE J. Biomed. Health Inf.* **23** 1990–2001
[7] Nakanishi M, Wang Y, Chen X, Wang Y-T, Gao X and Jung T-P 2018 Enhancing detection of SSVEPs for a high-speed brain speller using task-related component analysis *IEEE Trans. Biomed. Eng.* **65** 104–12
[8] Wong C M, Wan F, Wang B, Wang Z, Nan W, Lao K F, Mak P U, Vai M I and Rosa A 2019 Learning across multi-stimulus enhances target recognition methods in SSVEP-based BCIs *J. Neural Eng.* **17** 016026
[9] Yan W, Xu G, Xie J, Li M and Dan Z 2018 Four novel motion paradigms based on steady-state motion visual evoked potential *IEEE Trans. Biomed. Eng.* **65** 1696–704
[10] Yan W Q, Xu G H, Chen L T and Zheng X W 2019 Steady-state motion visual evoked potential (SSMVEP) enhancement method based on time-frequency image fusion *Comput. Intell. Neurosci.* **2019** 9439407
[11] Chen X, Wang Y, Zhang S, Gao S, Hu Y and Gao X 2017 A novel stimulation method for multi-class SSVEP-BCI using intermodulation frequencies *J. Neural Eng.* **14** 026013
[12] Chen X, Chen Z, Gao S and Gao X 2013 Brain–computer interface based on intermodulation frequency *J. Neural Eng.* **10** 066009
[13] Vialatte F B, Maurice M, Dauwels J and Cichocki A 2010 Steady-state visually evoked potentials: focus on essential paradigms and future perspectives *Prog. Neurobiol.* **90** 418–38
[14] Lin Z, Zhang C, Wu W and Gao X 2007 Frequency recognition based on canonical correlation analysis for SSVEP-based BCIs *IEEE Trans. Biomed. Eng.* **54** 1172–6
[15] Zhang Y, Dong L, Zhang R, Yao D, Zhang Y and Xu P 2014 An efficient frequency recognition method based on likelihood ratio test for SSVEP-based BCI *Comput. Math. Methods Med.* **2014** 908719
[16] Zhang Y, Xu P, Cheng K and Yao D 2014 Multivariate synchronization index for frequency recognition of

SSVEP-based brain–computer interface *J. Neurosci. Methods* **221** 32–40
[17] Chen X, Wang Y, Gao S, Jung T-P and Gao X 2015 Filter bank canonical correlation analysis for implementing a high-speed SSVEP-based brain–computer interface *J. Neural Eng.* **12** 046008
[18] Diez P F, Mut V A, Perona E M A and Laciar Leber E 2011 Asynchronous BCI control using high-frequency SSVEP *J. Neuroeng. Rehabil.* **8** 39
[19] Zhang Z, Li X and Deng Z 2010 A CWT-based SSVEP classification method for brain-computer interface system 2010 *Int. Conf. Intelligent Control and Information Processing (Dalian, China, 13–15 August 2010)* pp 43–48
[20] Nakanishi M, Wang Y, Wang Y-T and Jung T-P 2015 A comparison study of canonical correlation analysis based methods for detecting steady-state visual evoked potentials *PLoS One* **10** e0140703
[21] Nakanishi M, Wang Y, Wang Y-T, Mitsukura Y and Jung T-P 2014 A high-speed brain speller using steady-state visual evoked potentials *Int. J. Neural Syst.* **24** 1–19
[22] Zhang Y, Zhou G, Zhao Q, Onishi A, Jin J, Wang X and Cichocki A 2011 Multiway canonical correlation analysis for frequency components recognition in SSVEP-based BCIs *18th Int. Conf. on Neural Information Processing (ICONIP) (Shanghai, People's Republic of China, 13–17 November, 2011)* (Berlin: Springer) pp 287–95
[23] Zhang Y, Zhou G, Jin J, Wang X and Cichocki A 2014 Frequency recognition in SSVEP-based BCI using multiset canonical correlation analysis *Int. J. Neural Syst.* **24** 1450013
[24] Jiao Y, Zhang Y, Jin J and Wang X 2016 Multilayer correlation maximization for frequency recognition in SSVEP brain-computer interface *2016 6th Int. Conf. on Information Science and Technology (Dalian, People's Republic of China, 6–8 May 2016)* (IEEE) pp 31–35
[25] Zhang Y, Zhou G, Jin J, Wang X and Cichocki A 2015 SSVEP recognition using common feature analysis in brain–computer interface *J. Neurosci. Methods* **244** 8–15
[26] Wang H, Zhang Y, Waytowich N R, Krusienski D J, Zhou G, Jin J, Wang X and Cichocki A 2016 Discriminative feature extraction via multivariate linear regression for SSVEP-based BCI *IEEE Trans. Neural Syst. Rehabil. Eng.* **24** 532–41
[27] Zhou Z H, Wu J X and Tang W 2002 Ensembling neural networks: many could be better than all *Artif. Intell.* **174** 1570
[28] Xu M, Chen L, Zhang L, Qi H, Ma L, Tang J, Wan B and Ming D 2014 A visual parallel-BCI speller based on the time–frequency coding strategy *J. Neural Eng.* 11 026014
[29] Wang Y, Chen X, Gao X and Gao S 2017 A benchmark dataset for SSVEP-based brain–computer interfaces *IEEE Trans. Neural Syst. Rehabil. Eng.* **25** 1746–52